Jefferson Lab PAC 28 Letter of Intent

Charged Pion Electroproduction Ratios at High p_T

G.M. Huber[1]

[1] *University of Regina, Regina, SK S4S-0A2 Canada*

huberg@uregina.ca

(Dated: June 27, 2005)

Abstract

We propose a series of measurements of the $p(e,e'\pi^+)n$, $d(e,e'\pi^+)nn_{sp}$ and $d(e,e'\pi^-)pp_{sp}$ reactions, to determine the t-dependence of the π^-/π^+ ratio from nucleons. As $-t$ is increased, the hadronic interaction scale is reduced independently of the observation scale of the virtual photon. Thus, measurements of hard exclusive meson electroproduction at large $-t$ can provide valuable information about hard-scattering processes in general. The extraction of the π^-/π^+ ratio at high p_T is of particular interest because the ratio allows certain soft contributions to be divided out, allowing hard-scattering contributions to be more readily observable. This has been recently applied in exclusive pion photoproduction, where the π^-/π^+ at large p_T was found to be consistent with expectations based on hard gluon exchange. However, this handbag factorization calculation can not account for the size of the experimental cross sections, and so it is necessary to confirm this description with a complementary reaction. Exclusive pion electroproduction is an appropriate choice for this test, because the photon's hadronic component is rapidly suppressed with increasing Q^2. We propose measurements of the s-dependence of the π^-/π^+ ratio at constant θ^*, at $Q^2 = 2$ GeV^2 and $-t,-u > Q^2$. By taking data at two different values of ϵ, we can also investigate the relative contributions of longitudinal and transverse photons. Such measurements can be a valued tool to our better understanding of the relevant partonic degrees of freedom in the hard-scattering regime.

I. SCIENTIFIC MOTIVATION

The motivation of this letter is two-fold:

1. To measure the t-dependence of exclusive $\pi^{\pm}$ electroproduction from the nucleon so that we may gain a better understanding of hard scattering in terms of an appropriately chosen set of effective degrees of freedom. Presently, data only exist over a very limited range of Q^2 and $-t$.

2. While there has been much interest in the deep virtual factorization regime, the wide-angle factorization region is almost completely unexplored. We propose to measure $\pi^{\pm}$ electroproduction at fixed θ^* versus s at large $-t$ and $-u$ and fixed Q^2. By forming the differential cross section ratio π^-/π^+, certain nonperturbative contributions to the cross section may be divided out, allowing wide-angle factorization predictions to be more easily observed. At constant large θ^*, as s is increased we may expect the ratio to begin to follow hard scattering predictions.

The following sections describe the motivation in greater detail.

Study of Hard Scattering Mechanisms

Measurements of exclusive meson production are a useful tool in the study of hadronic structure. Through these studies one can discern the relevant degrees of freedom at different distance scales. In the transition region between low momentum transfer (where a description of hadronic degrees of freedom in terms of effective hadronic Lagrangians is valid) and large momentum transfer (where the degrees of freedom are quarks and gluons), t-channel exchange of a few Regge trajectories permits an efficient description of the energy dependence and the forward angular distribution of many real- and virtual-photon-induced reactions.

At center of mass scattering angles close to 90^o, photoproduction differential cross sections become nearly independent of t (plateau) and scale with energy according to the asymptotic quark counting rule [1] as s^{N-2}, where N is the number of active constitutents. This may be the domain where quark and gluon degrees of freedom dominate, but a quantitative understanding of experimental cross sections has been difficult to achieve. In the simplest

case, Compton scattering, perturbative calculations fall short by an order of magnitude for the cross section [2] and predict spin transfer coefficients with a sign opposite to experiment [3]. One is forced to rely on models based on effective partonic degrees of freedom relevant to the scale of observation.

There are a number of choices for the effective degrees of freedom. As an example, Regge trajectories are usually assumed to be linear in t, but when a model based on the extrapolation of linear Regge trajectories is applied to the high p_T region (large $-t$ and large $-u$), it fails to reproduce the photoproduction data [4]. One of the ways to reconcile, at higher momentum transfer, the Regge exchange model with experiment and the quark counting rules is to assume that the Regge trajectories saturate at -1 as $t \to -\infty$. This saturation of the Regge trajectories is closely related to the one-gluon exchange interaction between two quarks and follows from QCD-motivated models of the effective interquark potential [5, 6]. The resulting hard scattering amplitude leads to pion photoproduction differential cross sections which satisfy the quark counting rules and are in good agreement with differential cross sections at large p_T [4, 7]. Thus, saturated Regge trajectories are an economical way to deal with hard-scattering mechanisms.

The description of hard ω^0 electroproduction in terms of the effective degrees of freedom inherent in saturated Regge trajectories has also been successful [8]. In the case of electroproduction, one has access to two hard scales, as the observation scale of hadron structure $\lambda \sim 1/Q$ can be set independently of the interaction scale ($b \sim 1/\sqrt{-t}$). Furthermore, while the interaction of a real photon with nucleons is dominated by its hadronic component, this is rapidly suppressed with increasing Q^2. Thus, this two-handled probe is a valuable tool to place on solid ground the description of hard scatterings in terms of an appropriately chosen set of effective degrees of freedom. However, almost no high $-t$ electroproduction data exist. Our understanding of hard-scattering processes will benefit greatly if the t-dependency of the longitudinal and transverse parts of various meson electroproduction channels can be determined.

Applicability of QCD Factorization Theorems

One can also use hard exclusive processes to investigate the range of applicability of the QCD factorization theorems. The most important of these is the handbag factorization, where only one parton participates in the hard subprocess, and the soft physics is encoded in generalized parton distributions (GPDs). The handbag approach applies to deep exclusive meson production, where the photon has a large virtuality, Q^2, while the squared invariant momentum transfer, $-t$, is small [9, 10]. It also applies to wide-angle exclusive electroproduction, where $-t$ and $-u$ are large and Q^2 is less than $-t$ [11]. For wide-angle scattering, there is also an alternative scheme, leading-twist factorization, but this is not expected to be applicable until $-t \approx 10$ GeV^2 [12].

There are two significant differences between deep and wide-angle exclusive electroproduction of mesons. The first is that the handbag factorization is particularly simple in the wide-angle region. Instead of convolution as occurring in deep virtual processes, the wide-angle amplitudes appear as products of subprocess amplitudes and t-dependent form factors which represent $1/x$-moments of GPDs [11]. A second difference is that the deep virtual process is dominated by contributions from longitudinally polarized virtual photons for $Q^2 \to \infty$. Those from transverely polarized photons are suppressed by $1/Q^2$ and for these amplitudes factorization breaks down [13]. For wide-angle exclusive meson electroproduction, both photon polarizations contribute to the same twist order, so there is no break-down of factorization and the limit of small Q^2 is unproblematic [14]. However, it should be emphasized that for deep exclusive meson production, all order proofs of factorization exist [9], while for the wide-angle region factorization has only been shown to hold to leading order as yet [11].

While factorization tests of the deep exclusive meson production requires the 12 GeV upgrade or higher energies, the wide-angle region is of particular interest because of its accessibility with the JLab 6 GeV beam. Since a virtuality of $Q^2 = 2$ GeV^2 is easily obtained with 6 GeV electron beam, the main difficulty in accessing the large p_T region is presented by small exclusive cross sections, which are overcome by the high luminosity presently available at JLab. Thus, this is an experimental measurement which can be pursued immediately, in advance of the 12 GeV upgrade.

Measurements of the π^-/π^+ ratio

If the photon possessed definite isospin, the two reactions

$$\gamma^* n \to \pi^- p$$

$$\gamma^* p \to \pi^+ n$$

would be related to each other by simple isospin rotation and the cross sections would be equal [15]. However, interference terms between the isoscalar and isovector photon amplitudes have opposite signs for these processes, and these terms lead to a difference in the two cross sections.

Hadronic structure can also modify the ratio. In forward angle electroproduction, the charge of the pion acts as a tag on the flavor of the participating constituent. Applying isospin decomposition and charge symmetry invariance to s-channel knockout of valence quarks in the hard-scattering regime, O. Nachtmann [16] predicted the π^-/π^+ ratio to be

$$\frac{\gamma_T^* n \to \pi^- p}{\gamma_T^* p \to \pi^+ n} = \left(\frac{e_d}{e_u}\right)^2 = \frac{1}{4},$$

for transverse photons only.

The world data-set of π^-/π^+ ratios in which the longitudinal and transverse photon contributions are separated is shown in Fig. 1. These are preliminary data, which were taken to verify isovector dominance in the first pion form factor experiment, E93-021. At small $-t$, the longitudinal photon π^-/π^+ ratio is consistent with unity. At $Q^2 = 1.6$ GeV^2, the transverse photon π^-/π^+ ratio is much smaller, and are also consistent with linear (soft) Regge model predictions. Additional low $-t$ π^-/π^+ data from the second pion form factor experiment, E01-004, are still under analysis. No electroproduction data in the hard-scattering regime, where Nachtmann's predictions may be expected to apply, exist.

π^-/π^+ ratios from the $\gamma n \to \pi^- p$ and $\gamma p \to \pi^+ n$ reactions have also been measured at JLab [18, 19] using 1.1 to 5.5 GeV real photons. The experimental photoproduction cross sections are much larger than can be accounted for by one-hard-gluon-exchange diagrams in a handbag factorization calculation, even at $s \approx 10$ GeV^2 [14]. Either the vector meson dominance contribution is still large or the leading-twist generation of the meson underestimates the handbag contribution [12]. However, by forming the π^-/π^+ ratio the nonperturbative components represented by the form factors and meson distribution amplitude may be

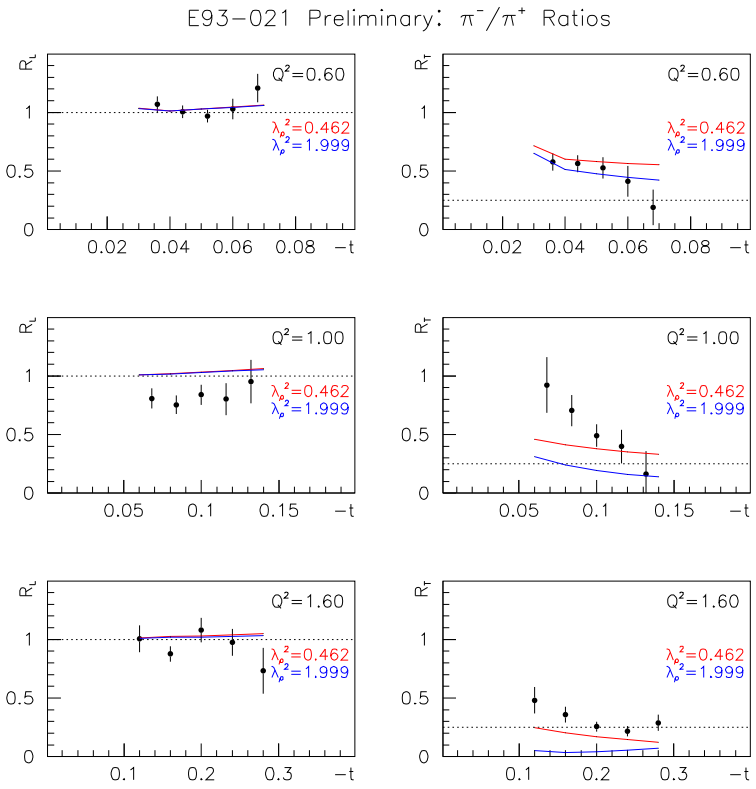

FIG. 1: Forward angle π^-/π^+ ratios at low $-t$. These are preliminary results from the first pion form factor experiment, E93-021 [17]. The red and blue curves are linear Regge model predictions.

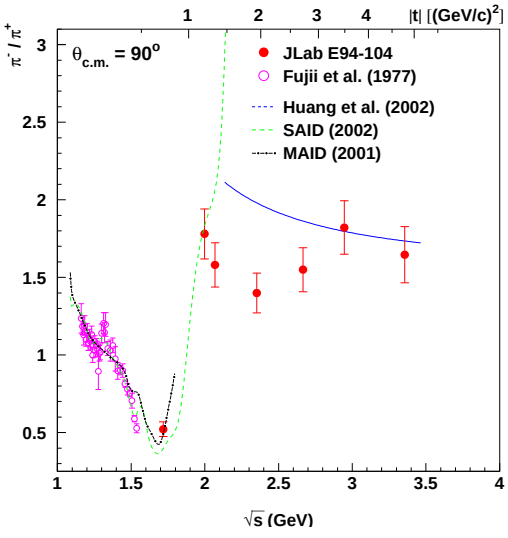

FIG. 2: $\theta^* = 90^o$ π^-/π^+ photoproduction ratios from Ref. [19]. The blue curve is the wide-angle factorization prediction.

divided out, allowing the perturbative contribution to be observed more readily. In the limit that the soft contributions are completely divided out, the one-hard-gluon-exchange calculation predicts [12] the simple scaling behavior

$$\frac{d\sigma(\gamma n \to \pi^- p)}{d\sigma(\gamma p \to \pi^+ n)} \approx \left[\frac{e_d(u-m_p^2)+e_u(s-m_p^2)}{e_u(u-m_p^2)+e_d(s-m_p^2)}\right]^2.$$

The recent JLab data at $\theta^* = 90^o$ and above $-t = 3$ GeV^2 are in agreement with the above expression (Fig. 2), while those at smaller θ^* are not [19].

While the π^-/π^+ photoproduction ratio at $\theta^* = 90^o$ appears to be in good agreement with the large-angle factorization prediction, this same calculation fails to describe the cross section. Therefore, the interpretation of this result is open to question and it should be confirmed with a complementary reaction. Since the hadronic component of the photon is suppressed in electroproduction approximately as $m_v^2/(Q^2+m_v^2)$, it is anticipated [14, 20] that the wide-angle factorization calculation will be in closer agreement with the data when Q^2 is larger than about 2 GeV^2, provided s, $-t$ and $-u$ are large. Thus, a measurement of the π^-/π^+ ratio in this kinematic regime is of definite interest. We propose to measure the s-dependence of this ratio at several θ^* to investigate the onset of scaling in this region. A preliminary calculation of the s-dependence of the π^-/π^+ ratio at $\theta^* = 90^o$, $Q^2 = 2$ GeV^2, $-t$,$-u > 2$ GeV^2 by H. Huang and P. Kroll [20] is shown in Fig. 3. Because of the contributions from both longitudinal and transverse photons, π^-/π^+ scaling is not as simple for electroproduction as it is for the case of photoproduction.

As part of the s-dependence study at fixed θ^*, we obtain the π^-/π^+ ratio versus $-t$ at a variety of W. Fig. 4 shows predicted π^-/π^+ ratios from the Regge model [4] versus $-t$ at fixed $Q^2 = 2.0$ GeV^2, W=2.1 GeV. The solid and dashed curves use linear (soft) and saturated (hard) Regge trajectories, respectively. Above $-t \approx 0.5$ GeV^2, the models are completely unconstrained by experimental data and the disagreement between the two Regge model descriptions, in particular for the π^-/π^+ ratios, is significant. This indicates that any ratio measurements at high $-t$ and $-u$ will be a sensitive measure of hard-scattering contributions and can be an effective tool for our better understanding of them.

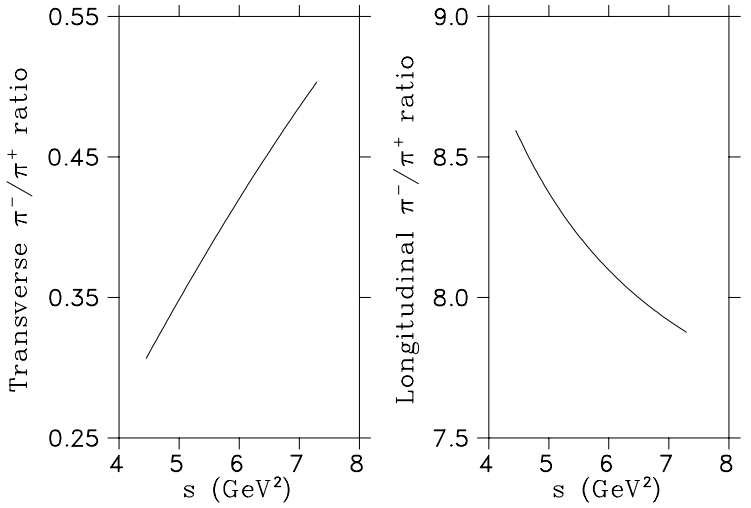

FIG. 3: Preliminary wide-angle factorization predictions of the s-dependence of the π^-/π^+ ratio at $Q^2 = 2$ GeV^2, $\theta^* = 90^o$ by H. Huang and P. Kroll [20].

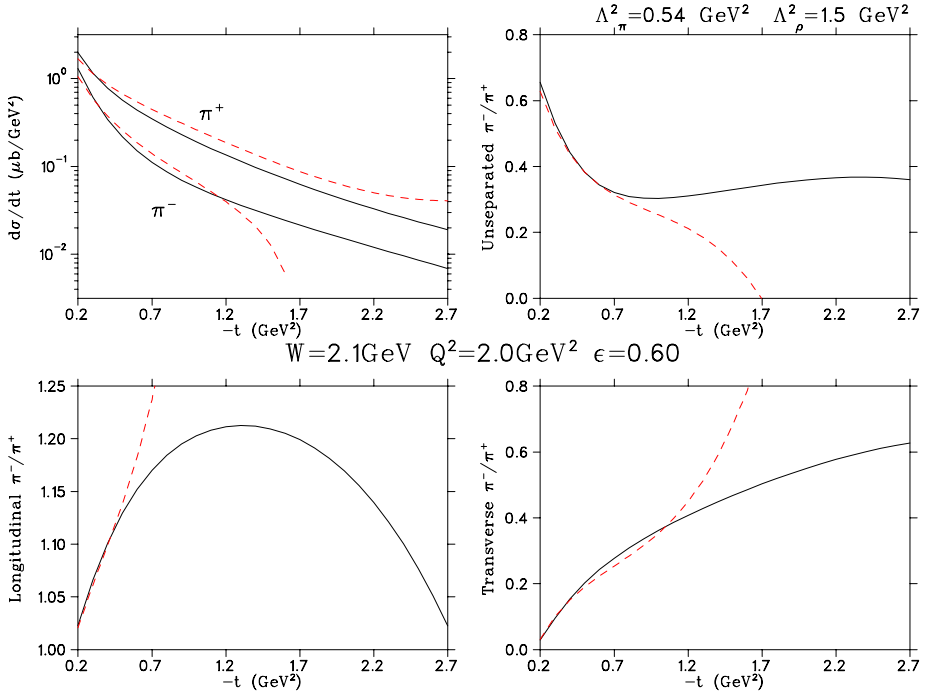

FIG. 4: Regge model predictions for π^-/π^+ ratios for scattering angles from $\theta^* = 0$ (left limit) to $\theta^* = 90^o$ (right limit). The solid curves use a linear (soft) Regge trajectory which is in agreement with experimental π^-/π^+ photoproduction ratios from 3.4-16 GeV[4]. The dashed curves [21] use the saturating (hard) Regge trajectory of Sergeenko [6] but are otherwise the same.

II. EXPERIMENT AND KINEMATICS

We propose measure of the $p(e,e'\pi^+)n$, $d(e,e'\pi^+)nn_{sp}$ and $d(e,e'\pi^-)pp_{sp}$ reactions above the resonance region, $W > 2$ GeV. The cross section of $n(e,e'\pi^-)p$ will be determined by the ratio method

$$d^4\sigma(\gamma^* n \to \pi^- p) = \frac{d^4\sigma(\gamma^* d \to \pi^- pp_{sp})}{d^4\sigma(\gamma^* d \to \pi^+ nn_{sp})} d^4\sigma(\gamma^* p \to \pi^+ n).$$

We have used this method in the E93-021 analysis shown in Fig. 1 and it works well.

Because the cross sections at high $-t$ are small, we have considered the two high luminosity halls A and C for this measurement. Hall A has the advantage of allowing > 2 GeV/c charged particle measurement for both the pion and the scattered electron, as well as a smaller experiment backlog, but the coincidence rate in Hall C is far larger, because of the larger solid angle and momentum acceptance of the SOS and HMS compared to the HRS[2]. Therefore, all further discussion shall assume that the experiment is performed in Hall C, with the scattered electron detected in the SOS and the pion in the HMS. There is sufficient missing mass resolution to guarantee the exclusivity of the reaction.

TABLE I: Proposed kinematics for the scan in s at fixed $\theta^* = 90^o$. For each setting listed here, six pion angle settings from $\theta^* = 0$ to 90^o would actually be taken.

$p(e,e'\pi^+)n$ kinematics for $Q^2 = 2.0$ GeV^2, $\theta^* = 90^o$									
$\sqrt{s}$ (GeV)	Beam (GeV)	$E_{e'}$ (GeV)	$\theta_{e'}$ (deg)	ϵ	θ_q (deg)	p_π (GeV)	θ_π (deg)	$-t$ (GeV^2)	$-u$ (GeV^2)
2.10	4.75	1.80	27.96	0.60	-14.99	1.56	-47.35	2.60	2.03
2.10	3.50	0.55	61.04	0.21	-8.53	1.56	-40.89	2.60	2.03
2.20	4.75	1.57	29.97	0.54	-13.08	1.68	-45.09	2.79	2.27
2.20	3.50	0.32	83.11	0.10	-5.32	1.68	-37.33	2.79	2.27
2.50	5.75	1.82	25.24	0.53	-10.73	2.09	-41.43	3.43	3.03
2.50	4.75	0.82	41.90	0.28	-7.57	2.09	-38.27	3.43	3.03
2.70	5.75	1.27	30.35	0.38	-7.84	2.38	-37.55	3.92	3.58
2.70	4.75	0.27	77.43	0.07	-3.20	2.38	-32.91	3.92	3.58

The wide-angle factorization regime requires $-t$ and $-u$ larger than 2 GeV^2. In addition, measurements at $Q^2 = 2$ GeV^2 or higher are desirable so that they will be complementary

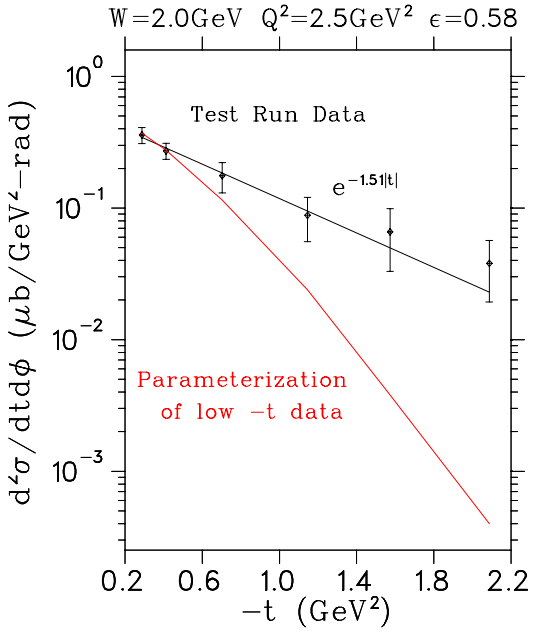

FIG. 5: Preliminary high $-t$ data taken during the second pion form factor experiment, E01-004, in order to constrain our parameterization of the $p(e,e'\pi^+)n$ cross section. These data were taken 10 hours of 4.7 GeV beam, and extend out to $\theta^* = 75^o$. At large $-t$, the experimental cross section is much larger than our previous data parameterization predicted.

to the $Q^2 = 0$ measurements and therefore provide a more effective test of the wide-angle factorization predictions for the π^-/π^+ ratio. These requirements are met by the $\theta^* = 90^o$ kinematics in Table 1. These settings can be obtained with 3, 4, 5 pass beam of a common linac gradient setting. For each entry in Table 1, we would actually take six pion angle settings, at $\theta^* = 0$, 15^o, 30^o, 50^o, 70^o and 90^o, in order to cover a large range in $-t$ and see at what angle the onset of scaling may occur.

Data rates at high $-t$ are largely unknown. However, during the second pion form factor experiment we took 10 hours of high $-t$ data, shown in Fig. 5, in order to constrain our parameterization of the $p(e,e'\pi^+)n$ cross section. Extrapolation of these data are used for the high ϵ beam-time estimate in Table 2 and the projected errors for the unseparated ratio obtained in Fig. 6. The low ϵ rates are expected to be small, so we only propose to take reduced statistics for two W scans.

TABLE II: Beam-time estimate for the proposed pion angle scans. For each $\sqrt{s}$, the majority of the beam-time is allocated to the $\theta^* = 90^o$ and 70^o pion angle settings.

		Beam hours per pion angle scan				
$\sqrt{s}$ (GeV)	ϵ	LH+ Hours	LD+ Hours	LD- Hours	Dummy Hours	Overhead Hours
High ϵ runs: 401 hrs (17 days)						
2.10	0.60	23	23	23	5	3
2.20	0.54	32	32	32	6	3
2.50	0.53	32	32	32	6	3
2.70	0.38	35	35	35	6	3
Low ϵ runs: 528 hrs (22 days)						
2.10	0.21	69	69	69	12	3
2.50	0.28	96	96	96	15	3

III. FURTHER STUDIES

Before submitting a full proposal, there is quite a bit more work that must be done.

1. We will have to decide the relative value of the low ϵ runs, given the difficulty and beam-time investment involved.

2. As we take data far from the q-vector, the azimuthal coverage becomes quite limited. Therefore, we will not be able to unambiguously separate the σ_{LT} and σ_{TT} contributions from σ_L. Our $\Delta\epsilon \sim 0.3$ leverage is otherwise acceptable, so we would be able to separate the ϵ-dependent and ϵ-independent contributions to the π^- and π^+ cross sections. and form separate ratios $(\pi^-/\pi^+)_{\epsilon-dependent}$ and $(\pi^-/\pi^+)_{\epsilon-independent}$.

   However, we may be able to do better than this. At small $-t$, we will be able to measure a wide range of ϕ, and separate σ_{LT} and σ_{TT} there, so perhaps with a model it may be possible to constrain the LT and TT contributions at large $-t$. If s-channel helicity conservation holds, these contributions are expected to be zero. We need to investigate these issues in much more detail before submitting a full proposal.

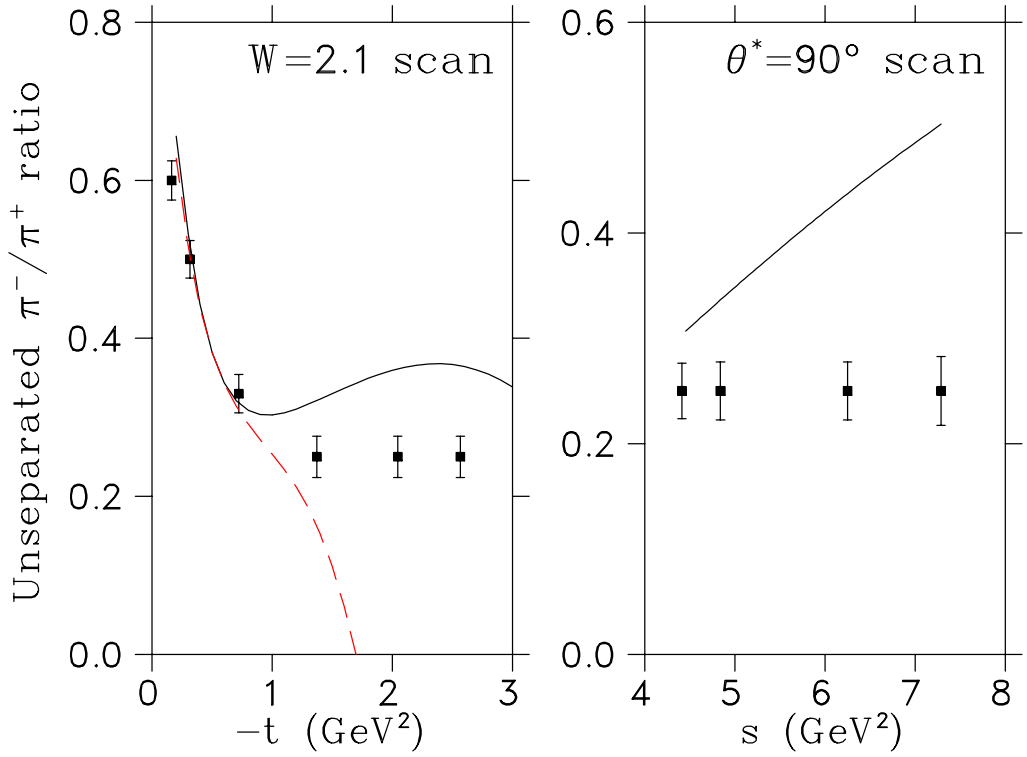

FIG. 6: Anticipated unseparated π^-/π^+ ratio errors, for the high ϵ kinematics listed in Table 1 and the 17 days of beam-time listed in Table 2. Separated π^-/π^+ ratios would be magnified by the $\Delta\epsilon \sim 0.3$ leverage. [Right:] In addition to the s-distribution shown at $\theta^* = 90^o$ at right, we would also obtain s-distributions at angles from $\theta^* = 0$-70^o, to see at what angle the factorization prediction may apply. The curve is the transverse π^-/π^+ ratio prediction by Huang and Kroll in Fig. 3. [Left:] In addition to the angular distribution shown at $W = 2.1$ GeV at left, we would also obtain distributions at $W = 2.2$, 2.5 and 2.7 GeV. The solid and dashed curves are the same Regge model calculations as in Fig. 4.

3. We also plan to study further optimization of the kinematics, rates, and expected errors.

Acknowledgements

The author wishes to thank H. Blok, D. Gaskell, J.M. Laget and P. Kroll for useful discussions and suggestions, M. Guidal for the saturated Regge model calculation and H.

Huang for the wide-angle factorization calculation.

---

[1] S.J. Brodsky, G.R. Farrar, Phys. Rev. Lett. **31** (1973) 1153.

[2] M. Vanderhaeghen, P. Guichon, J. Van de Wiele, Nucl. Phys. **22** (1997) 144C.

[3] C. Hyde-Wright et al, JLab Expt E99-114.

[4] M. Guidal, J.-M. Laget, M. Vanderhaeghen, Nucl. Phys. **A 627** (1997) 645.

[5] M. Brisudova et al., Phys. Rev. D **61** (2000) 054013.

[6] M.N. Sergeenko, Z. Phys. C **64** (1994) 315.

[7] M. Battaglieri, Phys. Rev. Lett. **90** (2003) 022002.

[8] J.M. Laget, Phys. Rev. D **70** (2004) 054023.

[9] J.C. Collins, L. Frankfurt, M. Strikman, Phys. Rev. D **56** (1997) 2982.

[10] M.I. Eides, L.L. Frankfurt, M.I. Strikman, Phys. Rev. D **59** (1999) 114025.

[11] H.W. Huang, R. Jakob, P. Kroll, K. Passek-Kumericki, Eur. Phys. J. C **33** (2004) 91.

[12] P. Kroll, hep-ph/0207118.

[13] L. Mankiewicz, G. Piller, Phys. Rev. D **61** (2000) 074013.

[14] H.W. Huang, P. Kroll, Eur. Phys. J. C **17** (2000) 423.

[15] A.M. Boyarski et al, Phys. Rev. Lett. **21** (1968) 1767.

[16] O. Nachtmann, Nucl. Phys. **B115** (1976) 61.

[17] V. Tadevosyan, private communication.

[18] L.Y. Zhu, et al., Phys. Rev. Lett. **91** (2003) 022003.

[19] L.Y. Zhu, et al., Phys. Rev. C **71** (2005) 044603.

[20] P. Kroll, H. Huang, private communication, 2005.

[21] M. Guidal, private communication, 2005.